

## Scalar triplet flavor leptogenesis with dark matter

Arghyajit Datta<sup>1,\*</sup>, Rishav Roshan<sup>2,†</sup> and Arunansu Sil<sup>1,‡</sup>

<sup>1</sup>*Department of Physics, Indian Institute of Technology Guwahati, Assam 781039, India*

<sup>2</sup>*Physical Research Laboratory, Ahmedabad—380009, Gujarat, India*



(Received 26 November 2021; accepted 9 May 2022; published 24 May 2022)

We investigate a simple variant of type-II seesaw, responsible for neutrino mass generation, where the particle spectrum is extended with one singlet right-handed neutrino and an inert Higgs doublet, both odd under an additional  $Z_2$  symmetry. While the role of the dark matter is played by the lightest neutral component of the inert Higgs doublet (IHD), its interaction with the Standard Model lepton doublets and the right-handed neutrino turns out to be crucial in generating the correct baryon abundance of the Universe through flavored leptogenesis from the decay of the  $SU(2)_L$  scalar triplet, involved in type-II framework. We observe a correlation between the smallness of the mass splitting, among the dark matter and the  $CP$ -odd neutral scalar from the IHD, and the largeness of the mass of the triplet followed from the dominance of the type-II mechanism over the radiative contribution to neutrino mass.

DOI: [10.1103/PhysRevD.105.095032](https://doi.org/10.1103/PhysRevD.105.095032)

### I. INTRODUCTION

Existence of tiny but non-zero neutrino mass [1–4] along with the observed excess of matter over antimatter in the Universe [5,6] are undoubtedly two of the most challenging problems in the present day particle physics and cosmology which signal for physics beyond the Standard Model (SM). Among many promising scenarios came up as a resolution to these issues, the seesaw mechanism provides an elegant framework to deal with. As is well known, in case of type-I seesaw [7–10], presence of SM singlet right handed neutrinos (RHN) not only helps in generating tiny neutrino mass but they can also be responsible for explaining the observed matter-antimatter asymmetry via leptogenesis [11–22]. A variant of it, namely the type-II seesaw construction [23–27] also provides an equally lucrative resolution by introducing a  $SU(2)_L$  scalar triplet to the SM field content whose tiny vacuum expectation value (vev) takes care of the small neutrino mass. However, to generate the baryon asymmetry of the Universe via leptogenesis, this minimal type-II framework needs to be extended either with another triplet [28–31] or by a singlet right-handed neutrino [32–37]. In the latter possibility, the role of the single RHN is to contribute to  $CP$  asymmetry generation

via the vertex correction (in the triplet decay) provided it carries a Yukawa interaction with the SM Higgs and lepton doublets.

Additionally, several astrophysical and cosmological observations indicate that energy budget of our Universe requires around 26% of non-baryonic matter, known as the dark matter (DM) [38–41]. To explain such DM, an extension of the SM is required as otherwise it fails to accommodate any such candidate from its own particle content. Since all these unresolved issues (tiny neutrino mass, matter-antimatter asymmetry and nature of dark matter) point out toward extension(s) of the SM, it is intriguing to establish a common platform for them. With this goal in mind, we focus on the SM extended with a scalar triplet and a fermion singlet (like one RHN). While this can explain the neutrino mass and matter-antimatter asymmetry as stated above, accommodating a DM in it is not that obvious. One simplest possibility emerges if that singlet fermion (the RHN) can be considered as the DM candidate. However, as pointed out above, this fermion taking part in the  $CP$  asymmetry generation has to carry an Yukawa interaction (of sizable strength) and hence cannot be stable provided its mass remains above the electroweak (EW) scale. On the other hand, if it happens to be lighter than the SM Higgs (or gauge bosons), it might be a freeze in type of DM [42]. In this case also, the small Yukawa coupling, as required by the freeze-in generation of DM relic, makes the  $CP$  asymmetry negligible and therefore such a possibility needs to be left out.

We thereby plan to extend this framework by including an inert Higgs doublet (IHD) [43–59] such that its lightest neutral component results in dark matter while the IHD too contributes to  $CP$  asymmetry generation via its Yukawa

\*datta176121017@iitg.ac.in

†rishav@prl.res.in

‡asil@iitg.ac.in

*Published by the American Physical Society under the terms of the Creative Commons Attribution 4.0 International license. Further distribution of this work must maintain attribution to the author(s) and the published article's title, journal citation, and DOI. Funded by SCOAP<sup>3</sup>.*

interaction involving the SM lepton doublet and the sole RHN. Involvement of the DM in generating the  $CP$  asymmetry required for explaining the matter-antimatter asymmetry of the Universe is an important aspect of our work. Note that the inert doublet DM phenomenology is mostly governed by the gauge interactions and the mass-splitting among the inert Higgs doublet components, but not on the Yukawa interaction [53] (contrary to the case of freeze-in RHN as DM) and hence it is not expected to be in conflict with sufficient production of  $CP$  asymmetry. Furthermore, search for doubly and singly charged particles involved in the triplet can be quite interesting from collider aspects. Keeping that in mind, we plan to keep the mass of the triplet not very heavy. It is further supported by the finding that the mass splitting among the IHD components (for DM relic satisfaction) along with the neutrino mass generation dominantly by the type-II mechanism keeps the triplet mass below  $10^{12}$  GeV. Note that it becomes essential to incorporate the flavor effects in leptogenesis [35,42,60–64] which come in to effect below the mass equivalent temperature  $\sim 10^{12}$  GeV. This observation, the importance of including flavor effects in triplet leptogenesis, is another salient feature of our analysis.

The paper is organized in the following manner. We introduce the structure of the model in Sec. II where the particle content with their respective charges under different symmetry group have been discussed. In Sec. III, we discuss the mechanism to generate the neutrino mass and how to get a complex structure of the Yukawa coupling matrix responsible for generating the matter-antimatter asymmetry. In Sec. IV, we briefly summarize the inert doublet DM phenomenology and move on to discuss generation of matter-antimatter asymmetry in the Universe via flavor leptogenesis in Sec. V. Finally in Sec. VI, we conclude.

## II. THE MODEL

The SM is extended with a  $SU(2)_L$  scalar triplet  $\Delta$ , a scalar doublet  $\Phi$ , and a fermionic SM singlet field  $N_R$ . The corresponding charge assignments of the relevant fields are provided in Table I. The Lagrangian involving the new fields is then given by

$$-\mathcal{L}_{\text{new}} = Y_\alpha \bar{\ell}_{L\alpha} \tilde{\Phi} N_R + Y_{\Delta\alpha\beta} \ell_{L\alpha}^T C i\tau_2 \Delta \ell_{L\beta} + \frac{1}{2} M_N \bar{N}_R^c N_R + \text{H.c.}, \quad (1)$$

where  $\alpha, \beta$  correspond to three flavor indices. Note that  $N_R$  and  $\Phi$  are odd under an additional discrete symmetry  $Z_2$ , thereby making  $\Phi$  as inert. This also forbids the Yukawa coupling of the SM Higgs with the RHN, however allows similar interaction with the inert Higgs doublet  $\Phi$ . The lightest neutral component of this  $\Phi$  field plays the role of the dark matter while decay of the triplet into lepton

TABLE I. Particles and their charges under different symmetries.

	$\ell_L$	$e_R$	$H$	$N_R$	$\Delta$	$\Phi$
$SU(2)_L$	2	1	2	1	3	2
$U(1)_Y$	$-\frac{1}{2}$	-1	$\frac{1}{2}$	0	1	$\frac{1}{2}$
$Z_2$	+	+	+	-	+	-

doublets generates the lepton asymmetry which will further be converted into baryon asymmetry by the sphaleron process. Here both the inert Higgs doublet and the RHN take part in producing the  $CP$  asymmetry.

The scalar sector of our model consists of the interaction involving the inert Higgs doublet  $\Phi$ , Higgs triplet  $\Delta$ , and the SM Higgs  $H$ . The most general scalar potential for the present scenario can be written as:

$$V(H, \Delta, \Phi) = V_H + V_\Delta + V_\Phi + V_{\text{int}}, \quad (2)$$

where

$$V_H = \mu_H^2 (H^\dagger H) + \lambda_H (H^\dagger H)^2, \quad (3a)$$

$$V_\Delta = M_\Delta^2 \text{Tr}(\Delta^\dagger \Delta) + \lambda_{\Delta 1} \text{Tr}(\Delta^\dagger \Delta)^2 + \lambda_{\Delta 2} [\text{Tr}(\Delta^\dagger \Delta)]^2, \quad (3b)$$

$$V_\Phi = \mu_\Phi^2 (\Phi^\dagger \Phi) + \lambda_\Phi (\Phi^\dagger \Phi)^2, \quad (3c)$$

$$\begin{aligned} V_{\text{int}} = & -\mu_1 (H^T i\tau_2 \Delta^\dagger H + \text{H.c.}) + \lambda_1 H^\dagger H \text{Tr}(\Delta^\dagger \Delta) \\ & + \lambda_2 H^\dagger \Delta \Delta^\dagger H + \lambda_3 H^\dagger \Delta^\dagger \Delta H \\ & + \lambda_4 (H^\dagger H) (\Phi^\dagger \Phi) + \lambda_5 (H^\dagger \Phi) (\Phi^\dagger H) \\ & + \left[ \frac{\lambda_6}{2} (H^\dagger \Phi)^2 + \text{H.c.} \right] - \mu_2 (\Phi^T i\tau_2 \Delta^\dagger \Phi + \text{H.c.}) \\ & + \lambda_7 \Phi^\dagger \Phi \text{Tr}(\Delta^\dagger \Delta) + \lambda_8 \Phi^\dagger \Delta \Delta^\dagger \Phi + \lambda_9 \Phi^\dagger \Delta^\dagger \Delta \Phi. \end{aligned} \quad (3d)$$

Here we consider all the parameters appearing in the scalar potential to be real. We also consider  $\mu_H^2 < 0$  as that would be crucial for electroweak symmetry breaking (EWSB). On the other hand, remaining mass parameters such as  $\mu_\Phi^2, M_\Delta^2$  are taken as positive. Denoting the vev of  $H$  and  $\Delta$  by  $v$  ( $= 246$  GeV) and  $v_\Delta$  respectively, the multiplets after the EWSB can be expressed as

$$\Phi = \begin{bmatrix} \Phi^+ \\ \frac{H_0 + iA_0}{\sqrt{2}} \end{bmatrix}, \quad H = \begin{bmatrix} 0 \\ \frac{v+h}{\sqrt{2}} \end{bmatrix}, \quad \Delta = \begin{bmatrix} \frac{\Delta^+}{\sqrt{2}} & \Delta^{++} \\ v_\Delta + \Delta^0 & -\frac{\Delta^-}{\sqrt{2}} \end{bmatrix}, \quad (4)$$

where  $h$  is the SM physical Higgs boson with mass 125.09 GeV [65] and the induced vev of the triplet is found to be related by [32]

$$v_\Delta \simeq \frac{v^2 \mu_1}{2M_\Delta^2}, \quad (5)$$

considering  $M_\Delta \gg v$ . Interestingly, the constraint on  $\rho$ -parameter ( $\rho = 1.00038 \pm 0.00020$ ) [66] restricts  $v_\Delta \lesssim 4.8$  GeV. Note that  $v_\Delta$  needs to be small enough to accommodate the tiny neutrino mass via  $\Delta \ell_L \ell_L$  coupling and hence we fix it at 1 eV. Then depending on the mass of the  $\Delta$  particle,  $\mu_1$  can be obtained by the use of Eq. (5). On the contrary, the analogous coupling  $\mu_2$  remains unrestricted and hence can have a sizable value. This therefore will be treated as independent parameter for generating sufficient  $CP$  asymmetry as we see in the leptogenesis section.

The masses of the different physical scalars of IHD are given (unaffected by the presence of the triplet scalar) as

$$\begin{aligned} m_{\Phi^\pm}^2 &= \mu_\Phi^2 + \lambda_1 \frac{v^2}{2}, \\ m_{H_0}^2 &= \mu_\Phi^2 + (\lambda_4 + \lambda_5 + \lambda_6) \frac{v^2}{2}, \\ m_{A_0}^2 &= \mu_\Phi^2 + (\lambda_4 + \lambda_5 - \lambda_6) \frac{v^2}{2}. \end{aligned} \quad (6)$$

with  $\lambda_L = \frac{\lambda_4 + \lambda_5 + \lambda_6}{2} > 0$ . Without any loss of generality, we consider  $\lambda_6 < 0$ ,  $\lambda_5 + \lambda_6 < 0$  so that the  $CP$  even scalar ( $H_0$ ) is the lightest  $Z_2$  odd particle and hence the stable dark matter candidate. Due to the presence of the term proportional to  $\mu_1$ , there will be a mixing between the SM Higgs

and the triplet. However, the mixing being of order  $v_\Delta$  (taken to be  $\sim 1$  eV, responsible to generate light neutrino mass), this can safely be ignored. We set  $\lambda_1, \lambda_2, \lambda_3 = 0$  for simplicity and then find masses of the physical triplet components as  $M_{\Delta^{\pm\pm}} \simeq M_{\Delta^\pm} \simeq M_{\Delta^0} \simeq M_\Delta$ . One should note that LHC puts a strong constraint on mass of  $\Delta^{\pm\pm}$  as  $M_{\Delta^{\pm\pm}} > 820$  GeV (870 GeV) at 95% confidence level (CL) from CMS [67] (ATLAS [68]) for  $v_\Delta \lesssim 10^{-4}$  GeV. LHC also set a constraints on  $M_{\Delta^\pm} > 350$  GeV.

### III. NEUTRINO MASS

We now proceed to discuss the neutrino mass generation in the present model. As mentioned before, the neutrino mass is expected to be generated via the triplet interaction with the SM lepton doublets resulting the type-II contribution as

$$m_\nu^{\text{II}} = 2Y_\Delta v_\Delta. \quad (7)$$

With a choice of  $v_\Delta$  as 1 eV, the coupling matrix  $Y_\Delta$  can be accordingly adjusted to produce the light neutrino matrix ( $m_\nu$ ) consistent with the oscillation data. To make it more specific, we consider,

$$m_\nu = m_\nu^{\text{II}} = U^* m_\nu^d U^\dagger, \quad (8)$$

with  $m_\nu^d = \text{diag}(m_1, m_2, m_3)$  and  $U$  is the Pontecorvo-Maki-Nakagawa-Sakata (PMNS) mixing matrix (in the charged lepton diagonal basis) of the form:

$$U = \begin{pmatrix} c_{12}c_{13} & c_{13}s_{12} & e^{-i\delta}s_{13} \\ -c_{23}s_{12} - e^{i\delta}c_{12}s_{13}s_{23} & c_{12}c_{23} - e^{i\delta}s_{12}s_{13}s_{23} & c_{13}s_{23} \\ s_{12}s_{23} - e^{i\delta}c_{12}c_{23}s_{13} & -e^{i\delta}c_{23}s_{12}s_{13} - c_{12}s_{23} & c_{13}c_{23} \end{pmatrix} \times \text{diag}(e^{i\alpha_1/2}, e^{i\alpha_2/2}, 1), \quad (9)$$

parametrized by three mixing angles  $\theta_{12}, \theta_{23}, \theta_{13}$  (denoted by  $c_{ij} = \cos \theta_{ij}, s_{ij} = \sin \theta_{ij}$ ), the Dirac  $CP$  phase  $\delta$  and Majorana  $CP$  phases ( $\alpha_1, \alpha_2$ ).

For simplicity, we now consider Majorana phases and the lightest neutrino mass to be zero. Thereby, using the best-fit values of the mixing angles and  $\delta$  [69] as in Table II, we obtain the following structure of the coupling matrix [using Eq. (7)] in case of normal hierarchy (NH) of neutrinos,

$$Y_\Delta = \left( \frac{1 \text{ eV}}{v_\Delta} \right) \times 10^{-3} \begin{pmatrix} 1.84 + 0.27i & -1.31 - 0.75i & -3.76 - 0.64i \\ -1.31 - 0.75i & 15.94 - 0.08i & 10.90 + 0.0038i \\ -3.76 - 0.64i & 10.90 + 0.0038i & 12.09 + 0.07i \end{pmatrix} \quad (10)$$

We will make use of this  $Y_\Delta$  in the rest of our analysis wherever appropriate.

Note that in our model, due to the presence of one RHN having Yukawa coupling  $Y$ , a radiative contribution to the light neutrino mass [70] is expected to be present which is given by

$$(m_\nu^{\text{R}})_{\alpha\beta} = \frac{Y_\alpha Y_\beta M_N}{32\pi^2} \left[ \frac{m_{H_0}^2}{m_{H_0}^2 - M_N^2} \ln \frac{m_{H_0}^2}{M_N^2} - \frac{m_{A_0}^2}{m_{A_0}^2 - M_N^2} \ln \frac{m_{A_0}^2}{M_N^2} \right]. \quad (11)$$

TABLE II. Neutrino mass and mixing parameters from the global fit [69] for NH.

Parameter	Best fit	$3\sigma$ range
$\Delta m_{21}^2 [10^{-5} \text{ eV}^2]$	7.50	6.94–8.14
$ \Delta m_{31}^2  [10^{-3} \text{ eV}^2]$	2.55	2.47–2.63
$\sin^2 \theta_{12}/10^{-1}$	3.18	2.71–3.69
$\sin^2 \theta_{23}/10^{-1}$	5.74	4.34–6.10
$\sin^2 \theta_{13}/10^{-2}$	2.200	2.000–2.405
$\delta/\pi$	1.08	0.71–1.99

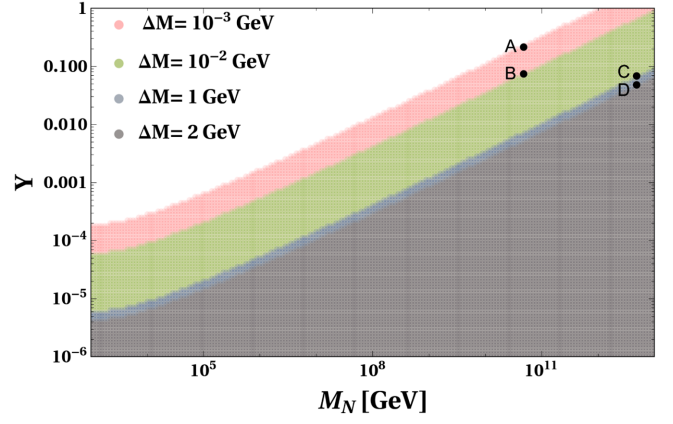
It is then understood that for a specific value of the DM mass,  $m_{H_0}$ , along with the mass splitting  $\Delta M = m_{\Phi^\pm} - m_{H_0} = m_{A_0} - m_{H_0}$ , and mass of the RHN, there is a contribution<sup>1</sup> to the light neutrino mass matrix which depends on the magnitude of  $Y_\alpha$  coupling. Since we plan to investigate the scenario where the light neutrino mass is mainly contributed by the type-II contribution, we determine here the limits on  $Y_\alpha$  for which  $m_\nu^R$  remains insignificant.

For this purpose, first we assume all  $Y_\alpha$  to be same given by  $Y$ . Second, we impose a restriction that the contribution to  $m_2$  (as  $m_2$  is the second lightest eigenvalue of  $m_\nu$ ) coming from  $m_\nu^R$  remains below 10% contribution followed from type-II seesaw estimate  $m_\nu^I$  (henceforth called type-II dominance). Using this ansatz, we provide  $Y$  versus  $M_N$  plot in Fig. 1 indicating an upper limit on  $Y$  value corresponding to a specific RHN mass. In making this plot, we consider DM mass  $m_{H_0} = 535$  GeV with different  $\Delta M$  indicated by different colors. This limit on  $Y$  will be useful in estimating the  $CP$  asymmetry. As the lightest neutrino is taken to be massless in type-II contribution, it is clear that with the appropriate  $Y$  value (consistent with the Fig. 1 and leptogenesis),  $m_1$  will defer from zero value as it obtains a tiny correction from  $m_\nu^R$ .

#### IV. DARK MATTER PHENOMENOLOGY

The present setup shelters two particles  $N_R$  and  $\Phi$  nontrivially charged under  $Z_2$ . Hence, being stable either of them can play the role of the DM. The phenomenology of a singlet fermions like  $N_R$  as a WIMP DM candidate with renormalizable interactions remain uninteresting as it predicts overabundant relic density due to the lack of their annihilation channels. On the other hand, as is well known, the study of an IHD provides several interesting prospects both in DM phenomenology as well as in collider searches and hence here we primarily stick to the IHD as dark matter by considering  $M_N > m_{H_0}$ . An unbroken  $Z_2$  symmetry in the current scenario guarantees the stability of the scalar

<sup>1</sup>Using the fact that  $M_N$  is very heavy compared to all IHD components, the radiative contribution can be approximated by  $(m_\nu^R)_{\alpha\beta} \simeq \frac{Y_\alpha Y_\beta}{32\pi^2} \frac{(m_{H_0} + m_{A_0})}{M_N} \Delta M [1 + \ln(\frac{m_{H_0}^2 + m_{A_0}^2}{2M_N^2})]$ .


 FIG. 1. Allowed range of  $Y$  against  $M_N$  to keep  $m_\nu^R$  subdominant compared to  $m_\nu^I$ .

dark matter. Since it is a well-studied framework, in this section we briefly focus on the parts of DM phenomenology relevant for our analysis extended to leptogenesis section.

#### A. Relic density

The inert Higgs doublet [43–52,54–56] extension of the SM is one of the simplest extension where a scalar multiplet can accommodate a DM candidate. Before going into the details of the DM phenomenology of IHD, we first briefly discuss the Boltzmann equation required to study the evolution of the DM in the Universe. DM ( $H_0$ ) being a part of a  $SU(2)_L$  doublet always remains in thermal equilibrium in early Universe due to its gauge and quartic interactions. The relic density of such a DM can be calculated by solving the Boltzmann equation

$$\frac{dY_{H_0}}{dz'} = -\frac{1}{z'^2} \langle \sigma v_{H_0 H_0 \rightarrow XX} \rangle (Y_{H_0}^2 - (Y_{H_0}^{\text{eq}})^2), \quad (12)$$

where  $z' = m_{H_0}/T$  and  $Y_{H_0}^{\text{eq}}$  denotes equilibrium number density of  $H_0$  whereas  $\langle \sigma v_{H_0 H_0 \rightarrow XX} \rangle$  represents the thermally averaged annihilation cross section [71] of the DM annihilating into the SM particles denoted by  $X$ . The relic density of the inert scalar  $H_0$  is then expressed as

$$\Omega_{H_0} h^2 = 2.755 \times 10^8 \left( \frac{m_{H_0}}{\text{GeV}} \right) Y_{H_0}^0, \quad (13)$$

with  $Y_{H_0}^0$  denoting the asymptotic abundance of the DM particle after freeze out. In order to calculate the relic density and study the DM phenomenology of the IHD dark matter we use the package micrOMEGAs4.3.5 [72].

As stated before, the case of an IHD dark matter is well studied and hence, we only summarize the results (in terms of relevant parameters) crucial for our analysis of baryon asymmetry of the Universe in the setup. To facilitate our discussion on DM, we provide a variation of the relic

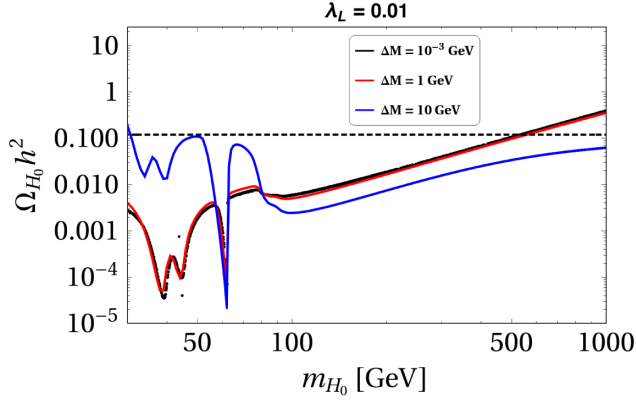


FIG. 2. Variation of the dark matter relic density ( $\Omega_{H_0} h^2$ ) with its mass ( $m_{H_0}$ ) for three different values of  $\Delta M$  while keeping  $\lambda_L = 0.01$ .

density of  $H_0$  ( $\Omega_{H_0} h^2$ ) with the dark matter mass ( $m_{H_0}$ ) for three different choices of mass splitting in Fig. 2. Here, one notices that in the mass range  $M_W \leq m_{H_0} < 500$  GeV (popularly known as the intermediate region), a typical feature of the IHD is observed where the relic abundance remains underabundant. The DM being a part of  $SU(2)_L$  doublet, it does annihilate and coannihilate to the SM gauge bosons with a large effective annihilation cross section resulting this underabundance in general. However, the correct relic density can still be produced for  $m_{H_0} \geq 535$  GeV with an appropriate choice of mass splitting  $\Delta M$  and Higgs portal coupling ( $\lambda_L$ ) as this leads to the cancellations among the  $s$ -channel,  $t$ -channel and the contact interaction involved in the scattering amplitude of the DM annihilating into the SM gauge bosons. In Fig. 2, one also notices that changing  $\Delta M$  from 1 GeV to  $10^{-3}$  GeV does not alter the relic result significantly. However, pushing  $\Delta M$  to a relatively larger value such as 10 GeV keeps the entire mass range of IHD as underabundant (except the Higgs resonance region). On the other hand, such a variation in  $\Delta M$  carries significant impact on the DM direct detection experiments as we see in the Sec. IV B below. Aside such dependence,  $\Delta M$  is also found to be restricted from the perturbativity point of view. As shown in [73], for  $\Delta M \gtrsim 20$  GeV, the IHD-Higgs coupling along with the Higgs quartic coupling become nonperturbative much before the Planck scale.

At this stage it is important to point out that the Yukawa interaction of the IHD with the SM leptons and the singlet fermion  $N_R$  [see Eq. (1)] does not alter the DM phenomenology of the IHD. Although it introduces an extra annihilation channel for IHD ( $t$ -channels mediated via  $N_R$  of SM leptons), its contribution remains suppressed due to the p-wave suppression. Even though, if this additional annihilation channel has a sizeable contribution to DM abundance compared to other channels, it does not help generate new allowed DM masses in the intermediate

mass regime of the IHD and hence remains uninteresting from the DM point of view.

## B. Direct and indirect detection

The null detection of the DM in direct search experiments like LUX [74], PandaX-II [75,76], and Xenon1T [77,78] puts a severe constraints on the DM parameter space. There exists two different possibilities for the DM to interact with nuclei at tree level in the scenario under consideration: (a) elastic scattering mediated by SM Higgs boson and (b) inelastic one mediated by electroweak gauge bosons. The spin independent elastic scattering cross section mediated by SM Higgs is given as [79]

$$\sigma^{\text{SI}} = \frac{\lambda_L^2 f_n^2 \mu_n^2 m_N^2}{4\pi m_h^4 m_{H_0}^2}, \quad (14)$$

where  $\mu_n = m_N m_{H_0} / (m_N + m_{H_0})$  is the DM-nucleon reduced mass and  $\lambda_L$  is the quartic coupling involved in DM-Higgs interaction. A recent estimate of the Higgs-nucleon coupling  $f$  gives  $f = 0.32$  [80]. On the other hand, the inelastic scattering cross section mediated by a gauge boson is expressed as [81],

$$\sigma_{\text{IE}}^{\text{SI}} = c \frac{G_F^2 m_N^2}{2\pi} Y^2 (\mathcal{N} - (1 - 4s_W^2) \mathcal{Z})^2 \quad (15)$$

with  $c = 1$  for fermions and  $c = 4$  for scalars. Here the hypercharge of the DM is  $1/2$ . Finally,  $\mathcal{N}$  and  $\mathcal{Z}$  represents the number of neutrons and protons respectively in the target nucleus with mass  $m_N$ . With  $\Delta M > 100$  keV [82], the inelastic scattering of DM with the nuclei is kinematically forbidden as the corresponding cross-section becomes larger than the average kinetic energy of the DM. While  $\Delta M \leq 100$  keV can rule out the entire sub-TeV mass regime of the DM even though allowed by the relic density as  $\sigma_{\text{IE}}^{\text{SI}} \simeq 4.9 \times 10^{-8}$  pb which is much larger than the constrained imposed by the Xenon1T experiment in a sub-TeV mass regime of the IHD dark matter.

Finally, one should also consider the indirect search experiments like Fermi-LAT [83], MAGIC [84] etc., which also provide promising detection prospects of the WIMP type DM. These experiments look for an excess of SM particles like photons and neutrinos in the Universe which can be produced from the annihilation or the decay of the DM. The present setup accommodates an IHD dark matter that can also produce such signals which can be detected in the indirect search experiments. The null detection of such signals so far can also constrain the DM parameter space. In a recent study [53], it has been shown that the IHD mass regime below 400 GeV is strictly ruled out by Fermi-LAT.

## V. LEPTOGENESIS

In this section, we aim to study the leptogenesis scenario resulting from the  $CP$  violating out of equilibrium decay of the triplet carrying lepton number of two units in the model. As advocated, this will happen due to the presence of the sole RHN of the setup contributing to the one-loop vertex correction to the tree level triplet decay into leptons as shown in Fig. 3. It is interesting to note that with one triplet, the generated  $CP$  asymmetry cannot be of purely flavored one [35] in contrast to the presence of this possibility in standard triplet leptogenesis involving two scalar triplets. We first discuss the generation of  $CP$  asymmetry from the triplet decay and then talk about the evolution of the lepton ( $B - L$ ) asymmetry using Boltzmann equations. In doing so, our plan is to keep the triplet mass as light as possible as that would be interesting from the point of view of collider search for triplet states. In turn, this indicates that flavor effects of the charged lepton Yukawa couplings need to be incorporated provided leptogenesis takes place below temperature  $\sim 10^{12}$  GeV.

### A. $CP$ asymmetry generation

The flavored  $CP$  asymmetry produced as a result of the interference between the tree level and the loop level diagram shown in Fig. 3 can be defined and evaluated as [32,33]

$$\begin{aligned} \epsilon_{\Delta}^{\ell_i} &= 2 \frac{\sum_j \Gamma(\bar{\Delta} \rightarrow \ell_i + \ell_j) - \Gamma(\Delta \rightarrow \bar{\ell}_i + \bar{\ell}_j)}{\Gamma_{\Delta}^{\text{tot}} + \Gamma_{\Delta}^{\text{tot}}}, \quad (16) \\ &= \frac{1}{4\pi} M_N \frac{\sum_j \text{Im}[\mu_2 Y_i Y_j (Y_{\Delta})_{ij}]}{\text{Tr}(Y_{\Delta}^{\dagger} Y_{\Delta}) M_{\Delta}^2 + |\mu_1|^2 + |\mu_2|^2} \log \left( 1 + \frac{M_{\Delta}^2}{M_N^2} \right), \quad (17) \end{aligned}$$

where,  $\Gamma_{\Delta}^{\text{tot}}$  is the total decay width of  $\Delta$ :

$$\begin{aligned} \Gamma_{\Delta}^{\text{tot}} &= \sum_{i,j} \Gamma(\Delta \rightarrow \bar{\ell}_i \bar{\ell}_j) + \Gamma(\Delta \rightarrow HH) + \Gamma(\Delta \rightarrow \Phi\Phi), \quad (18) \\ &= \frac{M_{\Delta}}{8\pi} \left[ \text{Tr}(Y_{\Delta}^{\dagger} Y_{\Delta}) + \frac{|\mu_1|^2 + |\mu_2|^2}{M_{\Delta}^2} \right]. \quad (19) \end{aligned}$$

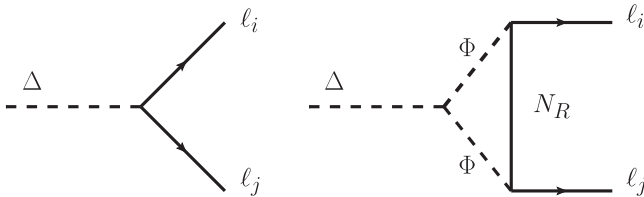


FIG. 3. The tree level and the vertex diagram required for the generation of  $CP$  asymmetry.

Similarly, the antitriplet decay  $\Gamma_{\Delta}^{\text{tot}}$  also contributes to the total decay width in the denominator. It would be useful to define the branching ratios  $B_{\ell}$ ,  $B_H$ , and  $B_{\Phi}$  at this stage, representative of the  $\Delta$  triplet decay to lepton and scalar final states as:

$$\begin{aligned} B_{\ell} &= \sum_{i=e,\mu,\tau} B_{\ell_i} = \sum_{i,j=e,\mu,\tau} B_{\ell_{ij}} = \sum_{i,j=e,\mu,\tau} \frac{M_{\Delta}}{8\pi\Gamma_{\Delta}^{\text{tot}}} |(Y_{\Delta})_{ij}|^2, \\ B_H &= \frac{|\mu_1|^2}{8\pi M_{\Delta} \Gamma_{\Delta}^{\text{tot}}}, \quad B_{\Phi} = \frac{|\mu_2|^2}{8\pi M_{\Delta} \Gamma_{\Delta}^{\text{tot}}}; \quad B_{\ell} + B_H + B_{\Phi} = 1. \quad (20) \end{aligned}$$

We notice now that among the various parameters involved in the expression of flavored  $CP$  asymmetry  $\epsilon_{\Delta}^{\ell_i}$  in Eq. (17),  $Y_{\Delta}$  is obtained from Eq. (10) while  $\mu_1$  becomes function of  $M_{\Delta}$  via Eq. (5) with the choice  $v_{\Delta} = 1$  eV. Finally, to maximize the  $CP$  asymmetry, we fix  $Y$  to its largest allowed value corresponding to a specific choice of  $M_N$  (and  $\Delta M$ ) from Fig. 1 so as to restrict the radiative contribution negligible (keeping it below 10%) compared to the type-II one toward light neutrino mass. Although there is no direct correlation between  $CP$  asymmetry and the mass splitting  $\Delta M$  among IHD components, it can be noted that  $\Delta M$  being involved in restricting the maximum value of  $Y$  for the type-II dominance of neutrino mass (see Fig. 1), plays an important role here. Hence,  $\epsilon_{\Delta}^{\ell_i}$  effectively remains function of three independent parameters  $\mu_2$ ,  $M_{\Delta}$  and  $M_N$ . It is interesting to note that in this case, there exists a coupling  $\mu_2$  in the  $CP$  asymmetry expression which does not participate in the neutrino mass generation unlike conventional type-(I + II) scenario where all the couplings involved in  $CP$  asymmetry also take part in the neutrino mass [32,33,37]. As a result, in the latter case (i.e., in type-(I + II) with type-II dominance, the relevant parameter space is restricted leading to  $M_{\Delta}$  quite heavy. For example, it was shown in [37], in the context of type-II-dominated left-right seesaw model, that  $M_{\Delta}$  turns out to be  $10^{12}$  GeV or beyond. On the other hand, involvement of otherwise free parameter  $\mu_2$  may open up a relatively wider parameter space in our case. Below we proceed to get some idea on the  $CP$  asymmetry generation by scanning over the parameters for our work.

Figure 4 shows the density contour plot for the absolute value of individual components of  $CP$  asymmetry in the  $M_{\Delta} - \mu_2$  plane while keeping  $M_N$  fixed at a specific value  $5 \times 10^{10}$  GeV. In producing these plots, we also consider two specific choices of  $\Delta M = 10^{-3}$  GeV (top panel) and  $\Delta M = 10^{-2}$  GeV (bottom panel). Benchmark points [A] and [B] are used to specify the values of Yukawa coupling  $Y$  for these mass splittings respectively (see Fig. 1). For  $M_{\Delta}$  below  $10^{11}$  GeV (though larger than  $10^9$  GeV), tau-Yukawa interaction comes to equilibrium making the asymmetries along  $a$  (a coherent superposition

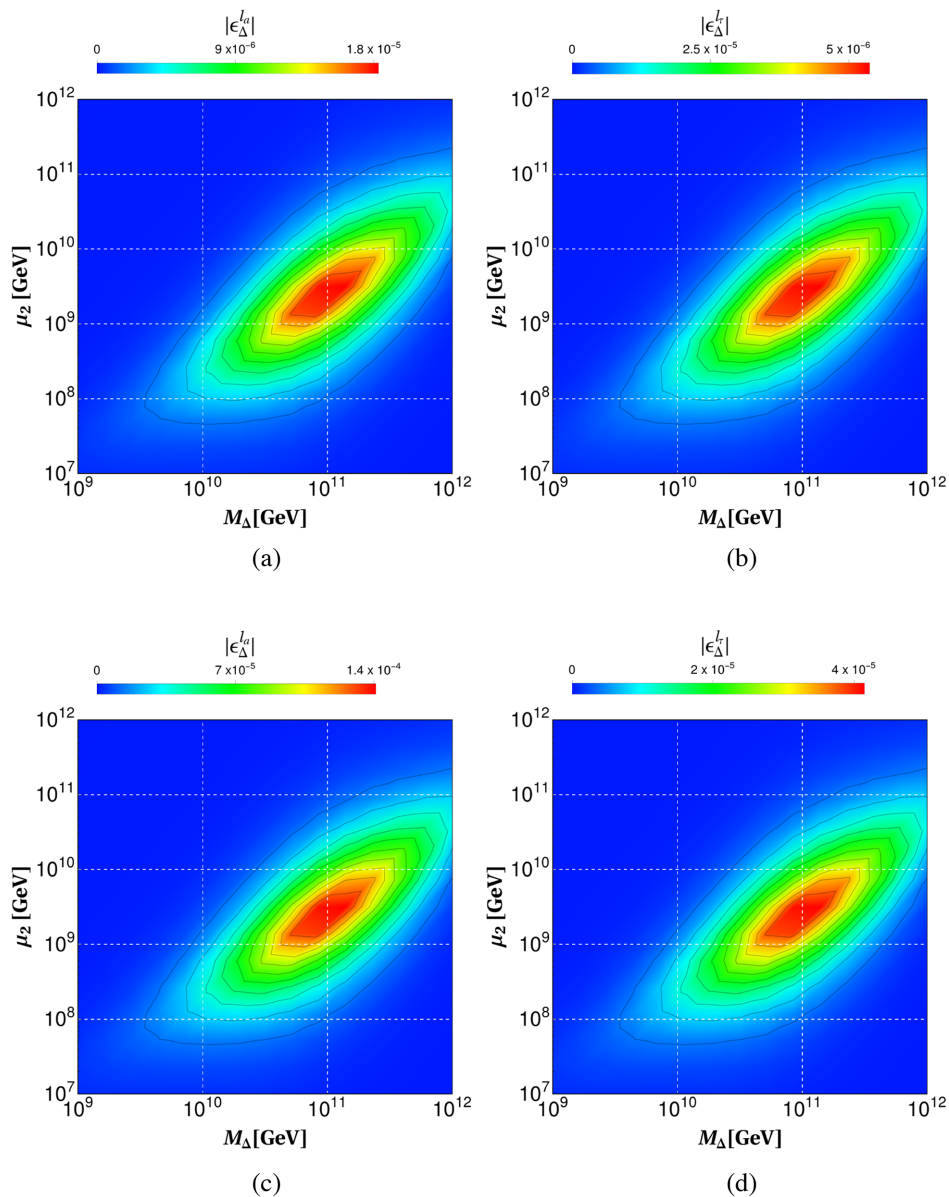


FIG. 4. Density contours of individual  $CP$  asymmetries in  $\mu_2 - M_\Delta$  plane for  $M_N = 5 \times 10^{10}$  GeV. Top panel: Left plot (a) and right plot (b) represent the density contours of  $|\epsilon_{\Delta}^{e a}|$  and  $|\epsilon_{\Delta}^{e \tau}|$  respectively with  $\Delta M = 10^{-3}$  GeV (using BP [A] from Fig. 1); Bottom panel: Left plot (c) and right plot (d) correspond to density contours of  $|\epsilon_{\Delta}^{e a}|$  and  $|\epsilon_{\Delta}^{e \tau}|$  respectively with  $\Delta M = 10^{-2}$  GeV (using BP [B] from Fig. 1).

of  $e$  and  $\mu$  lepton flavors) and  $\tau$  flavor distinguishable. We elaborate on it later. Hence in this region, we study  $\epsilon_{\Delta}^{e a, \tau}$  separately in Fig. 4(a) and (b) respectively. In the plot, the red (blue) region indicates the highest (lowest) absolute value of  $CP$  asymmetry while the green and the yellow regions indicate intermediate values of it. Maximum  $CP$  asymmetry<sup>2</sup> (the value of which is indicated in the top bar) results around the central region. Comparing the top and bottom panels of plots, we find that it is possible to generate relatively larger  $CP$  asymmetry once we lower  $\Delta M$ .

<sup>2</sup>For the present analysis, it turns out  $B_l \gg B_\phi$ .

However, we cannot keep on lowering  $\Delta M$  indefinitely ( $\Delta M$  below 100 keV is not feasible as we have discussed it in the DM section).

### B. Evolution of $B - L$ asymmetry

With the above estimates of the  $CP$  asymmetries in different flavor directions, we study here the evolution of  $B - L$  asymmetry via Boltzmann equations. It naturally involves all possible interactions with the thermal bath in the early Universe. As we aim here to bring down the leptogenesis scale (i.e., as low  $M_\Delta$  as possible) as stated earlier, the situation becomes more involved. Below the

energy scale  $M_\Delta \lesssim 10^{12}$  GeV, particularly in the temperature regime  $10^9$  GeV  $\lesssim T \lesssim 10^{12}$  GeV, along with bottom and charm quarks, tau Yukawa related interactions come to thermal equilibrium because of which the quantum coherence of lepton doublets is lost. As a result, in this regime, two orthogonal directions denoted by  $i = a$  (coherent superposition of  $e$  and  $\mu$  lepton flavors) and  $\tau$  survive. On the other hand, QCD instanton and EW sphaleron reactions also reach equilibrium at this temperature range making the baryon number as a nonconserved quantity, though it conserves the individual  $B/3 - L_i$  charges. So, an appropriate study of the evolution of the lepton asymmetry should be performed by knowing the evolution of the  $B/3 - L_i$  charges with  $i = a$  and  $\tau$ . Further below region of  $10^5$  GeV  $\lesssim T \lesssim 10^9$  GeV, strange quark and muon Yukawa interactions achieve thermal equilibrium indicating that the lepton doublets completely lose their quantum coherence. Hence, lepton asymmetry becomes distinguishable along all three flavors  $e$ ,  $\mu$ , and  $\tau$ . Below  $T < 10^5$  GeV, electron Yukawa reaches the equilibrium.

In order to study the evolution of the  $B - L$  asymmetry, we need to employ a set of coupled Boltzmann equations following the analysis of [35]. This set includes differential equations for triplet density  $\Sigma = \Delta + \bar{\Delta}$ , triplet asymmetry  $\Delta_\Delta = \Delta - \bar{\Delta}$ , and  $B/3 - L_i$  asymmetries considering flavor effects as we have considered a specific hierarchy  $M_\Delta < M_N$  in our analysis. Assuming the triplet scalar was at thermal equilibrium with plasma in the early Universe, below are the specified interactions which have the potential to change its number density as well as produce or washout the effective  $B - L$  charge asymmetry:

- (i) Decay [ $\Delta \rightarrow \bar{\ell}_i \bar{\ell}_j$ ,  $\Delta \rightarrow HH$  and  $\Delta \rightarrow \Phi\Phi$ ] and inverse decay: The total decay rate density is then represented by:  $\gamma_D = \gamma_D^\ell + \gamma_D^H + \gamma_D^\Phi$ , with  $\gamma_D = \frac{K_1(z)}{K_2(z)} n_\Sigma^{\text{Eq}} \Gamma_\Delta^{\text{Tot}}$ ,  $K_1(z)$ ,  $K_2(z)$  are the modified

Bessel functions. Here  $n_\Sigma^{\text{Eq}}$  is the equilibrium number density of  $\Sigma_\Delta$  and  $z$  is defined as  $M_\Delta/T$ .

- (ii) Gauge induced scatterings  $\Delta\Delta \leftrightarrow ff$ ,  $\Delta\Delta \leftrightarrow XX$  (s-channel),  $\Delta\Delta \leftrightarrow GG$  (triplet mediated t,u-channel, and four point vertex contributions), where  $f$  stands for SM fermions,  $G$  are SM Gauge bosons,  $X = H, \Phi$ . Altogether the reaction densities are characterized by  $\gamma_A$ , where  $\gamma_A = \frac{m_\Delta^4}{64\pi^4} \int_{x_{\min}}^\infty dx \sqrt{x} \frac{K_1(z\sqrt{x}) \hat{\sigma}_A}{z}$ ,  $x = s/M_\Delta^2$  ( $s$  is the center of mass energy). Here  $\hat{\sigma}_A$  is the reduced cross section inclusive of all gauge induced processes, where  $\hat{\sigma}$  is related to the usual cross section  $\sigma$  for a process [ $1 + 2 \rightarrow 3 + 4 + \dots$ ] by:  $\hat{\sigma} = \frac{8}{s} [(p_1 \cdot p_2)^2 - m_1^2 m_2^2] \sigma$  with  $p_1, p_2$  be the four momentum of initial particles having mass  $m_1, m_2$ .
- (iii) Lepton number ( $\Delta L = 2$ ) and Lepton flavor violating  $s$  and  $t$  channel scatterings (mediated by the triplet/anti-triplet):  $XX \leftrightarrow \bar{\ell}_i \bar{\ell}_j$ ,  $X\ell_j \leftrightarrow \bar{X} \bar{\ell}_i$  having reaction densities  $\gamma_{\ell_i \ell_j}^{XX}$  and  $\gamma_{X\ell_i}^{X\ell_j}$  respectively.
- (iv) Lepton flavor violating triplet mediated  $s$  and  $t$  channel scattering:  $(\ell_a \ell_b \leftrightarrow \ell_i \ell_j)_s$ ,  $(\ell_a \ell_b \leftrightarrow \ell_i \ell_j)_t$  with reaction densities given by  $(\gamma_{\ell_i \ell_j}^{\ell_a \ell_b})_s$  and  $(\gamma_{\ell_i \ell_j}^{\ell_a \ell_b})_t$ .

Keeping in mind the above discussion, the following Boltzmann equations are constructed,

$$sHz \frac{dY_\Sigma}{dz} = - \left( \frac{Y_\Sigma}{Y_\Sigma^{\text{Eq}}} - 1 \right) \gamma_D - 2 \left[ \left( \frac{Y_\Sigma}{Y_\Sigma^{\text{Eq}}} \right)^2 - 1 \right] \gamma_A, \quad (21)$$

$$sHz \frac{dY_{\Delta_\Delta}}{dz} = - \left[ \frac{Y_{\Delta_\Delta}}{Y_\Sigma^{\text{Eq}}} - \sum_k \left( \sum_i B_{\ell_i} C_{ik}^\ell - B_H C_k^H \right) \frac{Y_{X_k}}{Y_\Sigma^{\text{Eq}}} \right] \gamma_D, \quad (22)$$

$$\begin{aligned} sHz \frac{dY_{\Delta_{B/3-L_i}}}{dz} = & - \left( \frac{Y_\Sigma}{Y_\Sigma^{\text{Eq}}} - 1 \right) \epsilon_{\Delta_i}^\ell \gamma_D + 2 \sum_j \left( \frac{Y_{\Delta_\Delta}}{Y_\Sigma^{\text{Eq}}} - \frac{1}{2} \sum_k C_{ijk}^\ell \frac{Y_{X_k}}{Y_\Sigma^{\text{Eq}}} \right) B_{\ell_{ij}} \gamma_D \\ & - \sum_{j,k} \left\{ 2 \left( C_k^H + \frac{1}{2} C_{ijk}^\ell \right) (\gamma_{\ell_i \ell_j}^{HH} + \gamma_{H\ell_i}^{H\ell_j}) + C_{ijk}^\ell (\gamma_{\ell_i \ell_j}^{\Phi\Phi} + \gamma_{\Phi\ell_i}^{\Phi\ell_j}) \right\} \frac{Y_{X_k}}{Y_\Sigma^{\text{Eq}}} \\ & - \sum_{j,a,b,k} C_{ijabk}^\ell ((\gamma_{\ell_i \ell_j}^{\ell_a \ell_b})_s + (\gamma_{\ell_i \ell_j}^{\ell_a \ell_b})_t) \frac{Y_{X_k}}{Y_\Sigma^{\text{Eq}}}, \end{aligned} \quad (23)$$

where  $Y_{\Delta_x}$  is defined as the ratio between particle and antiparticle number densities difference to entropy:  $Y_{\Delta_x} = (n_x - n_{\bar{x}})/s$ , where  $n_x(n_{\bar{x}})$  is number density of a particular species  $X(\bar{X})$ .

Depending on the temperature range, the index  $i$  in the right-hand side (rhs) of Eq. (23) will run differently, e.g.,

for  $10^9$  GeV  $\lesssim T \lesssim 10^{12}$  GeV,  $i = a, \tau$  as done in Fig. 4, while for  $T < 10^9$  GeV,  $i = e, \mu, \tau$  need to be included. The generated asymmetry in number densities involving leptons of a specific flavor  $Y_{\Delta_{\ell_i}}$  as well as that of the Higgs (originated from the inverse decay and subtraction of the on-shell contribution for  $\Delta L = 2$  processes) can be related



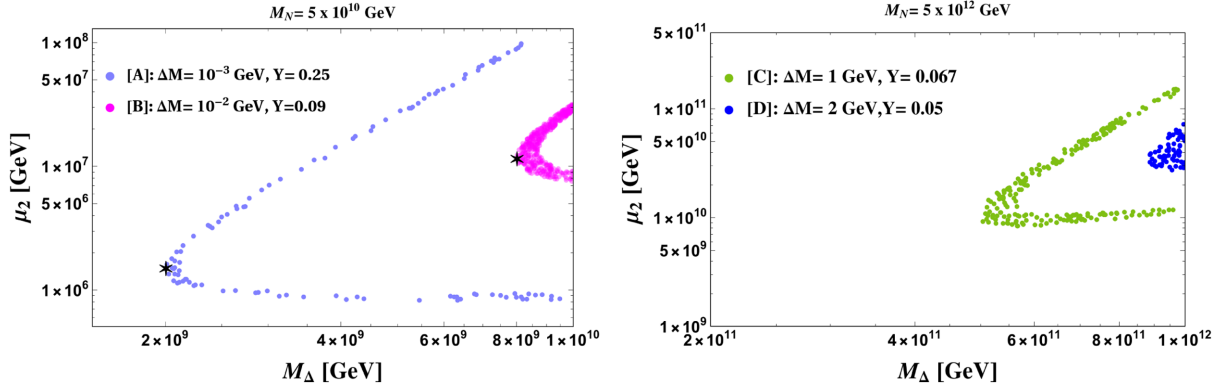


FIG. 5. Contour plots for final baryon asymmetry ( $Y_{\Delta_B} = (8.718 \pm 0.012) \times 10^{-11}$ ) in  $\mu_2 - M_\Delta$  plane. Left panel:  $M_N = 5 \times 10^{10}$  GeV while  $\Delta M = 10^{-3}$  GeV (light blue) and  $\Delta M = 10^{-2}$  GeV (magenta), Right panel:  $M_N = 5 \times 10^{12}$  GeV while  $\Delta M = 1$  GeV (light green) and  $\Delta M = 2$  GeV (blue).

to the fundamental asymmetries  $\Delta_\Delta$  and  $\Delta_{B/3-L_i}$  with the help of the equilibrium conditions applicable. The corresponding conversion factors<sup>3</sup> are defined in terms of  $C^\ell$  and  $C^H$  matrices as below [35,61]:

$$Y_{\Delta_{\ell_i}} = -\sum_k C_{ik}^\ell Y_{X_k} \quad \text{and} \quad Y_{\Delta_H} = -\sum_k C_k^H Y_{X_k}, \quad (24)$$

where  $Y_{X_k}$  are the elements<sup>4</sup> of  $Y_X^T = (Y_{\Delta_\Delta}, Y_{\Delta_{B/3-L_k}})$  and  $C_{ijk}^\ell$  and  $C_{ijabk}^\ell$  are given by:

$$C_{ijk}^\ell = C_{ik}^\ell + C_{jk}^\ell, \quad C_{ijabk}^\ell = C_{ik}^\ell + C_{jk}^\ell - C_{ak}^\ell - C_{bk}^\ell. \quad (25)$$

Then the final lepton asymmetry is converted to baryon asymmetry via sphaleron processes as given by:

$$Y_{\Delta_B} = 3 \times \frac{12}{37} \sum_i Y_{\Delta_{B/3-L_i}}, \quad (26)$$

where the factor 3 is due to the degrees of freedoms associated to the  $SU(2)_L$  scalar triplet.

### C. Results

In order to explore the parameter space of our model so as to produce the observed baryon asymmetry  $Y_{\Delta_B} = (8.718 \pm 0.012) \times 10^{-11}$  [85,86], first we choose a specific value of  $M_N = 5 \times 10^{10}$  GeV. Then based on our previous discussion we infer that lepton asymmetry with  $10^9$  GeV  $< M_\Delta < M_N$  will be produced along two orthogonal directions, i.e.,  $a$  and  $\tau$  while below  $10^9$  GeV, all three flavor

<sup>3</sup>We simplify the situation by considering the chemical potential of the  $\Phi$  field to be zero and hence corresponding  $C^\Phi$  does not appear.

<sup>4</sup>Here we take  $Y_{\Delta_\Delta} \equiv Y_{\Delta_{\Delta^0}} = Y_{\Delta_{\Delta^+}} = Y_{\Delta_{\Delta^{++}}}$  and  $Y_{\Delta_H} \equiv Y_{\Delta_{H^0}} = Y_{\Delta_{H^+}}$ .

directions have to be taken into account. With the help of chemical equilibrium constraint equations (coming from relevant Yukawa and EW sphaleron related reactions that are in equilibrium) as well as other constraints such as hypercharge conservation (applicable in this energy range) lead to the following structure of  $C^\ell$  and  $C^H$  matrices (for  $10^9$  GeV  $< M_\Delta < M_N$ ) [35,61]:

$$C^\ell = \frac{1}{718} \begin{pmatrix} -12 & 307 & -36 \\ 78 & -21 & 234 \end{pmatrix},$$

$$C^H = \frac{1}{359} \begin{pmatrix} 258 & 41 & 56 \end{pmatrix}. \quad (27)$$

For  $M_\Delta$  below  $10^9$  GeV,  $C^\ell$  and  $C^H$  become  $3 \times 4$  and  $1 \times 4$  matrices.

Using the input on the flavored  $CP$  asymmetries along  $a$  and  $\tau$  directions from Fig. 4, obtained as a function of  $\mu_2$  and  $M_\Delta$  for a specific  $\Delta M$  value, we employ the set of Boltzmann equations (21)–(23) while ignoring the last two

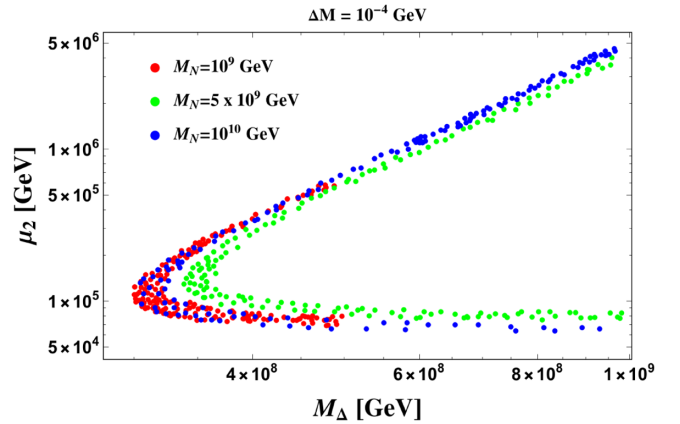


FIG. 6. Contour plots for final baryon asymmetry ( $Y_{\Delta_B} = (8.718 \pm 0.012) \times 10^{-11}$ ) in  $\mu_2 - M_\Delta$  plane for  $\Delta M = 10^{-4}$  while  $M_N = 10^{10}$  GeV (blue),  $M_N = 5 \times 10^9$  GeV (green) and  $M_N = 10^9$  GeV (red).

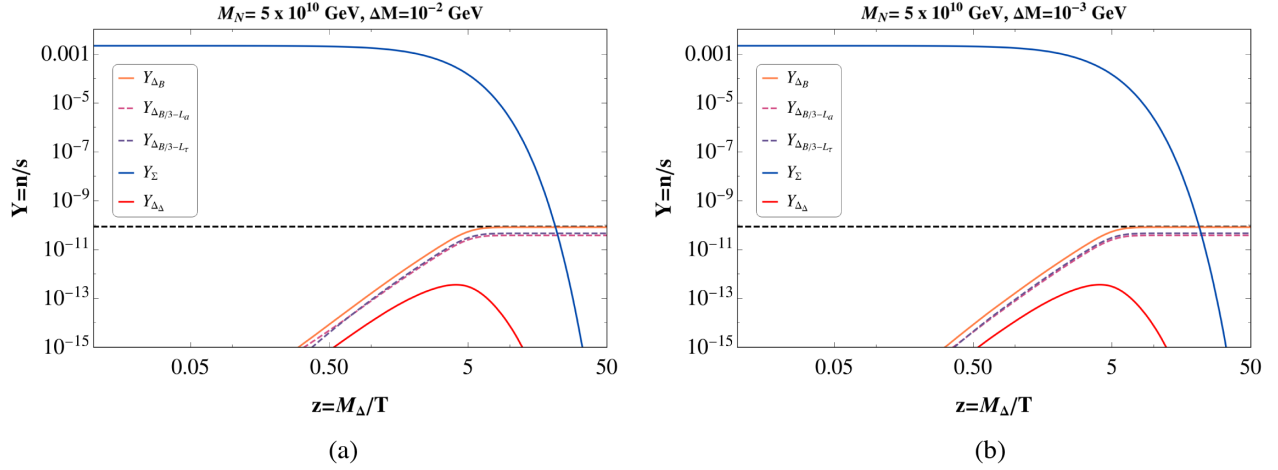


FIG. 7. Left panel (a) depicts the evolution of the comoving number density of individual components of lepton asymmetry together with the overall baryon asymmetry for  $M_\Delta = 8.02 \times 10^9$  GeV and  $\mu_2 = 1.14 \times 10^7$  GeV. Right panel (b) displays the same but for  $M_\Delta = 2.01 \times 10^9$  GeV and  $\mu_2 = 1.48 \times 10^6$  GeV. Evolution of comoving number density of  $\Sigma$ ,  $\Delta_\Delta$  are also shown on both the plots. The values of  $M_\Delta$  and  $\mu_2$  are obtained from the lowest allowed points of Fig. 5(a) (indicated by filled star).

terms of Eq. (23) to draw a contour plot for the correct final baryon asymmetry [via Eq. (26)] as shown in Fig. 5. The two contour plots, one in magenta and other in light blue patches, correspond to  $\Delta M = 10^{-2}$  GeV and  $10^{-3}$  GeV respectively. We therefore infer that the triplet can be as light as  $\sim 10^9$  GeV, contrary to the type-(I + II) case, which can successfully generate the required amount of baryon asymmetry, thanks to the flexibility involved due to the presence of parameter  $\mu_2$ .

We also notice that with the increase in  $\Delta M$  value, the baryon asymmetry satisfying contour gets shifted toward heavier mass range of the triplet. This observation is interesting as it is correlated to the DM phenomenology. We recall that even though a smaller  $\Delta M$  is not in conflict with the relic contribution to DM (in fact a relic satisfaction requires  $\Delta M$  below  $\mathcal{O}(1)$  GeV), it is actually restricted from below by the inelastic scattering of DM direct searches ( $\Delta M \gtrsim 10^{-4}$  GeV). On the other hand, the upper bound on  $\Delta M$  follows from the relic density satisfaction by the DM as can be seen from the Fig. 2. We find that with  $\Delta M = 1$  GeV (light green),  $M_\Delta$  can be as low as  $5 \times 10^{11}$  GeV, while a further increase in  $\Delta M$  such as 2 GeV (blue)<sup>5</sup> pushes the lightest possible  $M_\Delta$  value to  $9 \times 10^{11}$  GeV (while maintaining  $M_\Delta < M_N$ ) [see Fig. 5(b)]. As a result, we can work in the two flavor regime of leptogenesis with such  $\Delta M$  values. A further increase in  $\Delta M$  will take us to unflavored regime of leptogenesis. However, we refrain from considering a further larger values of  $\Delta M$  mainly because in that case, the relic density of the DM becomes underabundant. In Fig. 6, a similar contour plots are presented, but for fixed  $\Delta M = 10^{-4}$  GeV with different

<sup>5</sup>With such mass splitting, the DM having mass  $m_{H^0} = 535$  GeV can constitute  $\sim 83\%$  of the observed relic abundance.

$M_N$  values. As can be seen, the allowed mass of the triplet comes down to an even lower mass close to  $10^8$  GeV. It is perhaps pertinent here to mention that our entire parameter space corresponds to the Yukawa regime [34,35] where the Yukawa induced inverse decay processes (characterized by  $B_{\ell_{ij}}\gamma_D$ ) play an important role and hence flavor effects become crucial.

Hereafter, to show explicitly the various contributions of flavor in the evolution of  $Y_{\Delta_{B/3-L_i}}$  ( $i = a, \tau$ ), we pick up the lowest possible values of  $M_\Delta$  and corresponding  $\mu_2$  (for a fixed value of  $\Delta M = 10^{-2}$  GeV and  $M_N = 5 \times 10^{10}$  GeV) from Fig. 5(a). Then in Fig. 7(a), we show the evolution of number density to entropy ratio ( $Y = n/s$ ) for individual component of lepton asymmetries as well as the total baryon asymmetry with respect to  $z = M_\Delta/T$ . While plotting, we have assumed that initially  $\Delta(\bar{\Delta})$  were in equilibrium so  $\Delta_\Delta = 0$  and there were no lepton asymmetry. While the dark blue curve shows the evolution of  $\Sigma$ , abundances of  $B/3 - L_i$  asymmetries along individual flavor directions are shown in purple ( $a$  direction) and violet ( $\tau$  direction) dashed lines. The orange line stands for the evolution of the baryon asymmetry which asymptotically merges with the black dashed horizontal line indicative of the correct baryon asymmetry of the Universe.<sup>6</sup> Note

<sup>6</sup>In a recent work [31], authors have shown the importance of incorporating density matrix formalism to evaluate the baryon asymmetry for triplet leptogenesis, even beyond  $T \gtrsim 10^{12}$  GeV. In this formalism, diagonal entries of the density matrix indicate asymmetry along each lepton flavor direction while off-diagonal entries represent quantum correlations between different flavors. Though this is the most general approach, we have found that inclusion of the off-diagonal entries can only change the final result by 20% or less (corresponding to the values of parameters involved in producing the plots of Fig. 7) and hence neglected here.

that the dark blue curve starts to fall around  $z = 1$  due to the out of equilibrium decay of the triplet(anti-triplet) to different channels which in turn is reflected in the increase of lepton asymmetry (purple and violet-dashed lines). Around  $z = 5$ , the number density of the lepton asymmetry (in all directions) starts to saturate. The red curve shows the evolution of asymmetry generated in  $\Delta$  and  $\bar{\Delta}$  particles. Next in Fig. 7(b), the similar evolution of flavors ( $i = a, \tau$ ) becomes prominent once we choose the lowest possible value of  $M_\Delta$  corresponding to  $\Delta M = 10^{-3}$  GeV from Fig. 5(a).

Finally, we elaborate on how the mass-splitting  $\Delta M$  intervenes in different parts of the present work. Obviously,  $\Delta M$  has its most important role in DM phenomenology. As shown in Fig. 2, a value of  $\Delta M \sim \mathcal{O}(1)$  GeV or less is appropriate for having DM relic satisfaction having mass below TeV. Such a value therefore serves as the upper limit of  $\Delta M$  while it is bounded from below by  $\sim 10^{-4}$  GeV from the constraint on inelastic scattering amplitude of DM with detector nuclei. Turning into the neutrino part, we notice from Fig. 1 that in order to maintain the type-II dominance toward the neutrino mass, the maximum allowed value of neutrino Yukawa coupling  $Y$  has to be reduced with the increase of  $\Delta M$  for a specific choice of RHN mass  $M_N$ . On the other hand, a larger  $Y$  (and hence smaller  $\Delta M$ ) is favored from the point of view of enhancing the  $CP$  asymmetry with a specific  $M_N$ . Therefore a judicious choice has to be made for choosing  $\Delta M$  which not only be responsible for type-II dominance but also remains small enough so as to allow sufficient  $CP$  asymmetry. Such a choice has to be further guided by its upper ( $\sim \mathcal{O}(1)$  GeV) and lower ( $10^{-4}$  GeV) limits. With this entire viable range of  $\Delta M$ , masses of the RHNs are found to be in the regime  $\sim 10^{(9-12)}$  GeV.

## VI. CONCLUSION

In this work, we present a simple extension of the basic type-II seesaw (i.e., with one  $SU(2)_L$  triplet in addition to

SM) scenario including an additional RHN and one IHD, which can accommodate neutrino mass, dark matter as well as capable of explaining the baryon asymmetry of the Universe via leptogenesis mechanism. The interesting part of the study is the involvement of the DM multiplet, along with the RHN, in the vertex correction of the triplet's decay to two leptons which can successfully produce the required amount of  $CP$  asymmetry in order to address the baryon asymmetry of the Universe. Although the decay of RHN can also produce lepton asymmetry in the present setup, we assume a specific mass hierarchy  $M_\Delta < M_N$  and hence the asymmetry generated by the decay of the triplet is the effective one. We incorporate the flavor effects in this triplet leptogenesis study as we aim to lower the triplet mass as much as possible in view of its accessibility at the collider. We find it is possible to generate sufficient lepton asymmetry with  $M_\Delta$  as low as  $\sim 10^8$  GeV.

Turning to the neutrino side, where the dominant contribution to the light neutrino mass follows from the tiny vev of the triplet, there exists a radiative contribution too which we restrict to be negligible by choosing the associated Yukawa to be small enough. This consideration is related to the mass splitting involved in the IHD which plays a twofold role here. First, the IHD as a DM results with a specific range of this mass splitting ( $10^{-4} - \mathcal{O}(1)$  GeV). Second, a smaller mass splitting (hence a larger neutrino Yukawa) turns out to be preferable for generating sufficient  $CP$  asymmetry in this flavored leptogenesis framework. Since the lower limit of  $\Delta M$  is somewhat governed by the inelastic direct detection bound, in a way it restricts the mass of the triplet within a certain range.

On the other hand, due to the involvement of particles like  $\Delta^\pm$ ,  $\Delta^{\pm\pm}$ ,  $H^\pm$ , and  $N_R$ , the present setup is also subjected to the constraints coming from the lepton flavor violating decays like  $\mu \rightarrow e\gamma$ . Keeping this in our mind, we calculate the  $\text{Br}(\mu \rightarrow e\gamma)$  and found it to be many orders of magnitude smaller than that of the present upper bound on it ( $< 4.2 \times 10^{-13}$  at 90% CL [87]).

- 
- [1] Y. Fukuda *et al.* (Super-Kamiokande Collaboration), Evidence for Oscillation of Atmospheric Neutrinos, *Phys. Rev. Lett.* **81**, 1562 (1998).
  - [2] Q. Ahmad *et al.* (SNO Collaboration), Direct Evidence for Neutrino Flavor Transformation from Neutral Current Interactions in the Sudbury Neutrino Observatory, *Phys. Rev. Lett.* **89**, 011301 (2002).
  - [3] K. Eguchi *et al.* (KamLAND Collaboration), First Results from KamLAND: Evidence for Reactor Anti-Neutrino Disappearance, *Phys. Rev. Lett.* **90**, 021802 (2003).
  - [4] M. Ahn *et al.* (K2K Collaboration), Indications of Neutrino Oscillation in a 250 km Long Baseline Experiment, *Phys. Rev. Lett.* **90**, 041801 (2003).
  - [5] A. Riotto and M. Trodden, Recent progress in baryogenesis, *Annu. Rev. Nucl. Part. Sci.* **49**, 35 (1999).
  - [6] M. Dine and A. Kusenko, The origin of the matter—antimatter asymmetry, *Rev. Mod. Phys.* **76**, 1 (2003).
  - [7] P. Minkowski,  $\mu \rightarrow e\gamma$  at a rate of one out of  $10^9$  muon decays?, *Phys. Lett.* **67B**, 421 (1977).

- [8] M. Gell-Mann, P. Ramond, and R. Slansky, Complex spinors and unified theories, *Conf. Proc. C* **790927**, 315 (1979).
- [9] R. N. Mohapatra and G. Senjanovic, Neutrino Mass and Spontaneous Parity Nonconservation, *Phys. Rev. Lett.* **44**, 912 (1980).
- [10] J. Schechter and J. W. F. Valle, Neutrino masses in  $SU(2) \times U(1)$  theories, *Phys. Rev. D* **22**, 2227 (1980).
- [11] M. Fukugita and T. Yanagida, Baryogenesis without grand unification, *Phys. Lett. B* **174**, 45 (1986).
- [12] W. Buchmuller, P. Di Bari, and M. Plumacher, Leptogenesis for pedestrians, *Ann. Phys. (Amsterdam)* **315**, 305 (2005).
- [13] A. Anisimov, S. Blanchet, and P. Di Bari, Viability of Dirac phase leptogenesis, *J. Cosmol. Astropart. Phys.* **04** (2008) 033.
- [14] S. Davidson, E. Nardi, and Y. Nir, Leptogenesis, *Phys. Rep.* **466**, 105 (2008).
- [15] W. Buchmuller, R. Peccei, and T. Yanagida, Leptogenesis as the origin of matter, *Annu. Rev. Nucl. Part. Sci.* **55**, 311 (2005).
- [16] H. Davoudiasl and Y. Zhang, Baryon number violation via Majorana neutrinos in the early universe, at the LHC, and deep underground, *Phys. Rev. D* **92**, 016005 (2015).
- [17] N. Narendra, N. Sahoo, and N. Sahu, Dark matter assisted Dirac leptogenesis and neutrino mass, *Nucl. Phys.* **B936**, 76 (2018).
- [18] M. J. Dolan, T. P. Dutka, and R. R. Volkas, Dirac-phase thermal leptogenesis in the extended Type-I Seesaw model, *J. Cosmol. Astropart. Phys.* **06** (2018) 012.
- [19] S. Kashiwase and D. Suematsu, Baryon number asymmetry and dark matter in the neutrino mass model with an inert doublet, *Phys. Rev. D* **86**, 053001 (2012).
- [20] P. Konar, A. Mukherjee, A. K. Saha, and S. Show, A dark clue to seesaw and leptogenesis in a pseudo-Dirac singlet doublet scenario with (non)standard cosmology, *J. High Energy Phys.* **03** (2021) 044.
- [21] B. Barman, D. Borah, and R. Roshan, Nonthermal leptogenesis and UV freeze-in of dark matter: Impact of inflation reheating, *Phys. Rev. D* **104**, 035022 (2021).
- [22] S. Bhattacharya, R. Roshan, A. Sil, and D. Vatsyayan, Symmetry origin of baryon asymmetry, dark matter and neutrino mass, [arXiv:2105.06189](https://arxiv.org/abs/2105.06189).
- [23] R. N. Mohapatra and G. Senjanovic, Neutrino masses and mixings in gauge models with spontaneous parity violation, *Phys. Rev. D* **23**, 165 (1981).
- [24] G. Lazarides, Q. Shafi, and C. Wetterich, Proton lifetime and fermion masses in an  $SO(10)$  model, *Nucl. Phys.* **B181**, 287 (1981).
- [25] C. Wetterich, Neutrino masses and the scale of B-L violation, *Nucl. Phys.* **B187**, 343 (1981).
- [26] J. Schechter and J. W. F. Valle, Neutrino decay and spontaneous violation of lepton number, *Phys. Rev. D* **25**, 774 (1982).
- [27] B. Brahmachari and R. N. Mohapatra, Unified explanation of the solar and atmospheric neutrino puzzles in a minimal supersymmetric  $SO(10)$  model, *Phys. Rev. D* **58**, 015001 (1998).
- [28] E. Ma and U. Sarkar, Neutrino Masses and Leptogenesis with Heavy Higgs Triplets, *Phys. Rev. Lett.* **80**, 5716 (1998).
- [29] M. Senami and K. Yamamoto, Leptogenesis with supersymmetric Higgs triplets in TeV region, *Int. J. Mod. Phys. A* **21**, 1291 (2006).
- [30] R. Gonzalez Felipe, F. R. Joaquim, and H. Serodio, Flavoured  $CP$  asymmetries for type II seesaw leptogenesis, *Int. J. Mod. Phys. A* **28**, 1350165 (2013).
- [31] S. Lavignac and B. Schmauch, Flavour always matters in scalar triplet leptogenesis, *J. High Energy Phys.* **05** (2015) 124.
- [32] T. Hambye and G. Senjanovic, Consequences of triplet seesaw for leptogenesis, *Phys. Lett. B* **582**, 73 (2004).
- [33] T. Hambye, M. Raidal, and A. Strumia, Efficiency and maximal  $CP$ -asymmetry of scalar triplet leptogenesis, *Phys. Lett. B* **632**, 667 (2006).
- [34] T. Hambye, Leptogenesis: Beyond the minimal type I seesaw scenario, *New J. Phys.* **14**, 125014 (2012).
- [35] D. Aristizabal Sierra, M. Dhen, and T. Hambye, Scalar triplet flavored leptogenesis: A systematic approach, *J. Cosmol. Astropart. Phys.* **08** (2014) 003.
- [36] S. Mishra and A. Giri, Scalar triplet leptogenesis in the presence of right-handed neutrinos with  $S_3$  symmetry, *J. Phys. G* **47**, 055008 (2020).
- [37] T. Rink, W. Rodejohann, and K. Schmitz, Leptogenesis and low-energy  $CP$  violation in a type-II-dominated left-right seesaw model, *Nucl. Phys.* **B972**, 115552 (2021).
- [38] W. H. Julian, On the effect of interstellar material on stellar non-circular velocities in disk galaxies, *Astrophys. J.* **148**, 175 (1967).
- [39] M. Tegmark *et al.* (SDSS Collaboration), Cosmological parameters from SDSS and WMAP, *Phys. Rev. D* **69**, 103501 (2004).
- [40] C. L. Bennett *et al.* (WMAP Collaboration), Nine-year Wilkinson microwave anisotropy probe (WMAP) observations: Final maps and results, *Astrophys. J. Suppl. Ser.* **208**, 20 (2013).
- [41] D. Clowe, M. Bradac, A. H. Gonzalez, M. Markevitch, S. W. Randall, C. Jones, and D. Zaritsky, A direct empirical proof of the existence of dark matter, *Astrophys. J. Lett.* **648**, L109 (2006).
- [42] A. Datta, R. Roshan, and A. Sil, Imprint of the Seesaw Mechanism on Feebly Interacting Dark Matter and the Baryon Asymmetry, *Phys. Rev. Lett.* **127**, 231801 (2021).
- [43] L. Lopez Honorez, E. Nezri, J. F. Oliver, and M. H. G. Tytgat, The inert doublet model: An archetype for dark matter, *J. Cosmol. Astropart. Phys.* **02** (2007) 028.
- [44] L. Lopez Honorez and C. E. Yaguna, The inert doublet model of dark matter revisited, *J. High Energy Phys.* **09** (2010) 046.
- [45] A. Belyaev, G. Cacciapaglia, I. P. Ivanov, F. Rojas-Abatte, and M. Thomas, Anatomy of the inert two Higgs doublet model in the light of the LHC and non-LHC dark matter searches, *Phys. Rev. D* **97**, 035011 (2018).
- [46] S. Choubey and A. Kumar, Inflation and dark matter in the inert doublet model, *J. High Energy Phys.* **11** (2017) 080.

- [47] L. Lopez Honorez and C. E. Yaguna, A new viable region of the inert doublet model, *J. Cosmol. Astropart. Phys.* **01** (2011) 002.
- [48] A. Ilnicka, M. Krawczyk, and T. Robens, Inert doublet model in light of LHC run I and astrophysical data, *Phys. Rev. D* **93**, 055026 (2016).
- [49] A. Arhrib, Y.-L. S. Tsai, Q. Yuan, and T.-C. Yuan, An updated analysis of inert Higgs doublet model in light of the recent results from LUX, PLANCK, AMS-02 and LHC, *J. Cosmol. Astropart. Phys.* **06** (2014) 030.
- [50] Q.-H. Cao, E. Ma, and G. Rajasekaran, Observing the dark scalar doublet and its impact on the standard-model Higgs boson at colliders, *Phys. Rev. D* **76**, 095011 (2007).
- [51] E. Lundstrom, M. Gustafsson, and J. Edsjo, The inert doublet model and LEP II limits, *Phys. Rev. D* **79**, 035013 (2009).
- [52] M. Gustafsson, S. Rydbeck, L. Lopez-Honorez, and E. Lundstrom, Status of the inert doublet model and the role of multileptons at the LHC, *Phys. Rev. D* **86**, 075019 (2012).
- [53] D. Borah and A. Gupta, New viable region of an inert Higgs doublet dark matter model with scotogenic extension, *Phys. Rev. D* **96**, 115012 (2017).
- [54] J. Kalinowski, W. Kotlarski, T. Robens, D. Sokolowska, and A. F. Zarnecki, Benchmarking the inert doublet model for  $e^+e^-$  colliders, *J. High Energy Phys.* **12** (2018) 081.
- [55] A. Bhardwaj, P. Konar, T. Mandal, and S. Sadhukhan, Probing inert doublet model using jet substructure with multivariate analysis, *Phys. Rev. D* **100**, 055040 (2019).
- [56] D. Borah, R. Roshan, and A. Sil, Minimal two-component scalar doublet dark matter with radiative neutrino mass, *Phys. Rev. D* **100**, 055027 (2019).
- [57] S. Bhattacharya, P. Ghosh, A. K. Saha, and A. Sil, Two component dark matter with inert Higgs doublet: Neutrino mass, high scale validity and collider searches, *J. High Energy Phys.* **03** (2020) 090.
- [58] S. Bhattacharya, N. Chakrabarty, R. Roshan, and A. Sil, Multicomponent dark matter in extended  $U(1)_{B-L}$ : Neutrino mass and high scale validity, *J. Cosmol. Astropart. Phys.* **04** (2020) 013.
- [59] N. Chakrabarty, R. Roshan, and A. Sil, Two component doublet-triplet scalar dark matter stabilising the electroweak vacuum, [arXiv:2102.06032](https://arxiv.org/abs/2102.06032).
- [60] A. Abada, S. Davidson, F.-X. Josse-Michaux, M. Losada, and A. Riotto, Flavor issues in leptogenesis, *J. Cosmol. Astropart. Phys.* **04** (2006) 004.
- [61] E. Nardi, Y. Nir, E. Roulet, and J. Racker, The importance of flavor in leptogenesis, *J. High Energy Phys.* **01** (2006) 164.
- [62] S. Blanchet and P. Di Bari, Flavor effects on leptogenesis predictions, *J. Cosmol. Astropart. Phys.* **03** (2007) 018.
- [63] P. S. B. Dev, P. Di Bari, B. Garbrecht, S. Lavignac, P. Millington, and D. Teresi, Flavor effects in leptogenesis, *Int. J. Mod. Phys. A* **33**, 1842001 (2018).
- [64] A. Datta, B. Karmakar, and A. Sil, Flavored leptogenesis and neutrino mass with  $A_4$  symmetry, *J. High Energy Phys.* **12** (2021) 051.
- [65] D. de Florian *et al.* (LHC Higgs Cross Section Working Group Collaboration), *Handbook of LHC Higgs Cross Sections: 4. Deciphering the Nature of the Higgs Sector* (CERN, Geneva, 2017), Vol. 2.
- [66] P. A. Zyla *et al.* (Particle Data Group Collaboration), Review of particle physics, *Prog. Theor. Exp. Phys.* **2020**, 083C01 (2020).
- [67] A. M. Sirunyan *et al.* (CMS Collaboration), Combined measurements of Higgs boson couplings in proton–proton collisions at  $\sqrt{s} = 13$  TeV, *Eur. Phys. J. C* **79**, 421 (2019).
- [68] M. Aaboud *et al.* (ATLAS Collaboration), Measurements of Higgs boson properties in the diphoton decay channel with  $36 \text{ fb}^{-1}$  of  $pp$  collision data at  $\sqrt{s} = 13$  TeV with the ATLAS detector, *Phys. Rev. D* **98**, 052005 (2018).
- [69] P. F. de Salas, D. V. Forero, S. Gariazzo, P. Martínez-Miravé, O. Mena, C. A. Ternes, M. Tórtola, and J. W. F. Valle, 2020 global reassessment of the neutrino oscillation picture, *J. High Energy Phys.* **02** (2021) 071.
- [70] A. Ahriche, A. Jueid, and S. Nasri, Radiative neutrino mass and Majorana dark matter within an inert Higgs doublet model, *Phys. Rev. D* **97**, 095012 (2018).
- [71] P. Gondolo and G. Gelmini, Cosmic abundances of stable particles: Improved analysis, *Nucl. Phys.* **B360**, 145 (1991).
- [72] D. Barducci, G. Belanger, J. Bernon, F. Boudjema, J. Da Silva, S. Kraml, U. Laa, and A. Pukhov, Collider limits on new physics within micrOMEGAs\_4.3, *Comput. Phys. Commun.* **222**, 327 (2018).
- [73] A. Dutta Banik, R. Roshan, and A. Sil, Neutrino mass and asymmetric dark matter: Study with inert Higgs doublet and high scale validity, *J. Cosmol. Astropart. Phys.* **03** (2021) 037.
- [74] D. S. Akerib *et al.* (LUX Collaboration), Results from a Search for Dark Matter in the Complete LUX Exposure, *Phys. Rev. Lett.* **118**, 021303 (2017).
- [75] A. Tan *et al.* (PandaX-II Collaboration), Dark Matter Results from First 98.7 Days of Data from the PandaX-II Experiment, *Phys. Rev. Lett.* **117**, 121303 (2016).
- [76] X. Cui *et al.* (PandaX-II Collaboration), Dark Matter Results From 54-Ton-Day Exposure of PandaX-II Experiment, *Phys. Rev. Lett.* **119**, 181302 (2017).
- [77] E. Aprile *et al.* (XENON Collaboration), First Dark Matter Search Results from the XENON1T Experiment, *Phys. Rev. Lett.* **119**, 181301 (2017).
- [78] E. Aprile *et al.* (XENON Collaboration), Dark Matter Search Results from a One Ton-Year Exposure of XENON1T, *Phys. Rev. Lett.* **121**, 111302 (2018).
- [79] R. Barbieri, L. J. Hall, and V. S. Rychkov, Improved naturalness with a heavy Higgs: An Alternative road to LHC physics, *Phys. Rev. D* **74**, 015007 (2006).
- [80] J. Giedt, A. W. Thomas, and R. D. Young, Dark Matter, the CMSSM and Lattice QCD, *Phys. Rev. Lett.* **103**, 201802 (2009).
- [81] M. Cirelli and A. Strumia, Minimal dark matter: Model and results, *New J. Phys.* **11**, 105005 (2009).
- [82] C. Arina, F.-S. Ling, and M. H. G. Tytgat, IDM and iDM or the inert doublet model and inelastic dark matter, *J. Cosmol. Astropart. Phys.* **10** (2009) 018.
- [83] B. Eiteneuer, A. Goudelis, and J. Heisig, The inert doublet model in the light of Fermi-LAT gamma-ray data: A global fit analysis, *Eur. Phys. J. C* **77**, 624 (2017).

- [84] M. L. Ahnen *et al.* (MAGIC, Fermi-LAT Collaborations), Limits to dark matter annihilation cross-section from a combined analysis of MAGIC and Fermi-LAT observations of dwarf satellite galaxies, *J. Cosmol. Astropart. Phys.* **02** (2016) 039.
- [85] R. H. Cyburt, B. D. Fields, K. A. Olive, and T.-H. Yeh, Big bang nucleosynthesis: 2015, *Rev. Mod. Phys.* **88**, 015004 (2016).
- [86] N. Aghanim *et al.* (Planck Collaboration), Planck 2018 results. VI. Cosmological parameters, *Astron. Astrophys.* **641**, A6 (2020).
- [87] A. M. Baldini *et al.* (MEG Collaboration), Search for the lepton flavour violating decay  $\mu^+ \rightarrow e^+\gamma$  with the full dataset of the MEG experiment, *Eur. Phys. J. C* **76**, 434 (2016).